THE JOURNAL OF BIOLOGICAL CHEMISTRY VOL. 282, NO. 46, pp. 33284–33295, NOVEMBER 16, 2007

Identification of a Novel Inhibitor of Differentiation-1 (ID-1) Binding Partner, Caveolin-1, and Its Role in Epithelial-Mesenchymal Transition and Resistance to Apoptosis in Prostate Cancer Cells*[S]

Received for publication, June 21, 2007, and in revised form, September 10, 2007 Published, JBC Papers in Press, September 12, 2007, DOI 10.1074/jbc.M705089200

Xiaomeng Zhang[‡], Ming-Tat Ling[‡], Qi Wang[‡], Chi-Keung Lau[§], Steve C. L. Leung[‡], Terence K. Lee[§], Annie L. M. Cheung[‡], Yong-Chuan Wong[‡1], and Xianghong Wang[‡2]

From the Cancer Biology Group, the Departments of [‡]Anatomy and [§]Surgery, Faculty of Medicine, Pokfulam, University of Hong Kong, Hong Kong, Special Administrative Region, China

Recently, *ID-1* (inhibitor of differentiation/DNA binding) is suggested as an oncogene and is reported to promote cell proliferation, invasion, and survival in several types of human cancer cells through multiple signaling pathways. However, how Id-1 interacts with these pathways and the immediate downstream effectors of the Id-1 protein are not known. In this study, using a yeast two-hybrid screening technique, we identified a novel Id-1-interacting protein, caveolin-1 (Cav-1), a cell membrane protein, and a positive regulator of cell survival and metastasis in prostate cancer. Using an immunoprecipitation method, we found that the helix-loop-helix domain of the Id-1 protein was essential for the physical interaction between Id-1 and Cav-1. In addition, we also demonstrated that the physical interaction between Id-1 and Cav-1 played a key role in the epithelial-mesenchymal transition and increased cell migration rate as well as resistance to taxol-induced apoptosis in prostate cancer cells. Furthermore, our results revealed that this effect was regulated by Id-1-induced Akt activation through promoting the binding activity between Cav-1 and protein phosphatase 2A. Our study demonstrates a novel Id-1 binding partner and suggests a molecular mechanism that mediates the function of Id-1 in promoting prostate cancer progression through activation of the Akt pathway leading to cancer cell invasion and resistance to anticancer drug-induced apoptosis.

Id-1 (inhibitor of differentiation and DNA binding) is a member of the helix-loop-helix (HLH)[3] transcription factor family. It lacks a basic domain for DNA binding; therefore, it acts as a dominant inhibitor of the basic HLH transcription factors by forming heterodimers. Id-1 has multiple functions, including inhibition of differentiation, induction of proliferation, and delaying replicative senescence (1). In addition, *ID-1* has been suggested as a potential oncogene, because it is up-regulated in many types of human cancer such as breast (2), pancreas (3), cervical (4), and prostate cancers (5). Id-1 expression levels are positively associated with poor clinical outcome and drug resistance (4, 6, 7). For example, early stage cervical cancer patients with increased Id-1 expression show poor prognosis (4). In breast and ovarian cancer patients, enhanced Id-1 expression is correlated with more aggressive behavior as well as much shorter overall survival (6, 7). These lines of evidence suggest that Id-1 plays a positive role in promoting the development and progression of human cancer.

In addition to its well described role in cell proliferation (8, 9), recently, Id-1 has been reported to promote survival and metastatic ability of cancer cells. For example, overexpression of the Id-1 protein enhances invasive properties of hematopoietic cell lines through transactivation of the matrix metalloproteinase 9 transcription (10). In addition, Id-1 mediates transforming growth factor-β-induced epithelial mesenchymal transition (EMT), a process by which epithelial cells obtain mesenchymal features and show reduced cell-cell contact and motility, and is suggested to play a critical role during invasion and metastasis (11). Constitutive expression of the *ID-1* promoter as a result of loss of the NF-1/Rb/HDAC-1 transcription repressor complex is also found in metastatic breast cancer cells (12). Previously, we have observed in prostate cancer cells that ectopic expression of Id-1 promotes the growth of endothelial cells (13), suggesting its positive role in promoting angiogenesis. Recently, we and others have demonstrated that Id-1 is able to protect cancer cells against a variety of anticancer drug-induced apoptosis in several types of human cancer cells, including cervical, breast, prostate, and nasopharyngeal carcinomas (14). These results

* This work was supported by the Association for International Cancer Research, UK (to X. W.), and Research Grants Council HKU7470/04M (to Y. C. W.). The costs of publication of this article were defrayed in part by the payment of page charges. This article must therefore be hereby marked "*advertisement*" in accordance with 18 U.S.C. Section 1734 solely to indicate this fact.

The nucleotide sequence(s) reported in this paper has been submitted to the GenBank™/EBI Data Bank with accession number(s) NM_001753.

[S] The on-line version of this article (available at http://www.jbc.org) contains supplemental Figs. S1–S3.

[1] To whom correspondence may be addressed: Dept. of Anatomy, University of Hong Kong,1/F, Faculty of Medicine Bldg., 21 Sassoon Rd., Hong Kong, China. Tel.: 852-2819-2868; Fax: 852-2817-0857; E-mail: ycwong@hkucc.hku.hk.

[2] To whom correspondence may be addressed: xhwang@hkucc.hku.hk.

[3] The abbreviations used are: HLH, helix-loop-helix; Cav-1, caveolin-1; EMT, epithelial mesenchymal transition; RT, reverse transcription; HA, hemagglutinin; TRITC, tetramethylrhodamine isothiocyanate; MAPK, mitogen-activated protein kinase; ERK, extracellular signal-regulated kinase; MEK, MAPK/ERK kinase; MTT, 3-(4,5-dimethylthiazol-2-yl)-2,5-diphenyltetrazolium bromide; PI3K, phosphatidylinositol 3-kinase; PARP, poly(ADP-ribose) polymerase; PP2A, protein phosphatase 2A; PI3K, phosphatidylinositol 3-kinase.

are consistent with the reports on breast and gastric cancers that increased Id-1 expression is associated with highly aggressive phenotypes in both cell lines and animal models (15, 16). In combination with the evidence that Id-1 overexpression is frequently found in advanced cancers (6, 7), it is possible that the positive role of Id-1 in cancer metastasis and survival may provide an advantage for the progression of human cancer leading to poor clinical outcome.

Several signaling pathways have been suggested to mediate the function of Id-1. For example, the Id-1-induced invasion ability in breast cancer cells is mediated through induction of the expression of a 120-kDa gelatinase, a type IV collagenase matrix metalloproteinase family member (17). Matrix metalloproteinase 9 activation is found to be responsible for the Id-1-induced increased invasive ability in leukemia cells (10), suggesting that Id-1 plays a positive role in activation of the cell-matrix adhesion signaling pathway. In addition, Id-1 has been reported to be involved in the down-regulation of E-cadherin expression and reorganization of β-catenin and F-actin as well as in transforming growth factor-β-induced EMT in several cell types (11, 18), suggesting that it promotes metastatic ability through modification of the cell adherens junction complex. On the other hand, Id-1 is able to protect anticancer drug-induced apoptosis through activation of NF-κB and Raf/MEK and suppression of JNK pathways in prostate cancer and other types of cancer cells (19–22), indicating its ability to regulate multiple cell signaling pathways. However, it remains unknown as how Id-1 interacts with these pathways and what are the immediate downstream effectors of the Id-1 protein that mediate its interaction with cell signaling pathways. In this study, we report that by using yeast two-hybrid screening technique, we identified a novel Id-1 interacting protein, caveolin-1 (Cav-1), an integral cell membrane protein that interacts with multiple signaling molecules and regulates signaling transduction (23). In addition, we found that the HLH domain of the Id-1 protein was responsible for the interaction between Id-1 and Cav-1. We also demonstrate that the physical interaction between Id-1 and Cav-1 was essential for the positive role of Id-1 in inducing EMT and cell survival in prostate cancer cells. Furthermore, our results suggested that the Id-1-induced Akt activation through promoting the binding activity between Cav-1 and PP2A was accountable for its function as a promoter of prostate cancer cell invasion and resistance to anticancer drug-induced apoptosis.

EXPERIMENTAL PROCEDURES

Yeast Two-hybrid Screening for Id-1 Binding Candidates—A cDNA library was established from a human nonmalignant prostatic epithelial cell line, Hpr-1 (24), and cloned into the prey vector pGAD424, using the SMART™ cDNA library construction kit (Clontech). The full-length *ID-1* cDNA was cloned into the bait vector pAS2-1. The bait and prey constructs were co-transfected into the *Saccharomyces cerevisiae* strain CG-1945 using the YEASTMAKER™ yeast transformation system 2 kit (Clontech). Positive clones were selected in the medium-stringency medium, SD/−His/−Leu/−Trp, and galactosidase assay using the MATCHMAKER GAL4 two-hybrid system 3 and Libraries kit (Clontech). The positive plasmids were recovered using a plasmid extraction kit (YEASTMAKER™ yeast plasmid isolation kit, Clontech), transformed into *Escherichia coli* for plasmid amplification and sequencing for identity, respectively.

Cell Culture and Drugs—Two human prostate cancer cell lines, LNCap, obtained from American Type Culture Collection (Manassas, VA), and 22RV1, kindly provided by Prof. F. L. Chan (Chinese University of Hong Kong), were maintained in RPMI 1640 medium (Sigma) supplemented with 5 or 10% (v/v) fetal calf serum, respectively, penicillin (100 units/ml), and streptomycin (100 μg/ml) at 37 °C, 5% CO_2. The anti-cancer drug, taxol, PI3K/Akt specific inhibitors, LY294002 and wortmannin (Calbiochem; dissolved in Me_2SO), were diluted in culture medium to obtain the desired concentrations.

Plasmids and Transient Transfection—HA-tagged *CAV-1* was generated using the following primers: forward, 5′-ATTA GGA TCC ATG TCT GGG GGC AAA TAC-3′, and reverse, 5′-ATTA GGA TCC ATG TAC CCA TAC GAT GTT CCA GAT TAC GCT TCT GGG GGC AAA TAC GTA G-3′. The PCR products were then cloned into the pcDNA3.1 vector. The vector expressing the FLAG-tagged wild type Id-1 (*WT-ID-1*) was described previously (25), and FLAG-tagged truncated *ID-1* vectors were generated from the *WT-ID-1* and then cloned into the pcDNA3.1 vector. The vectors expressing FLAG-tagged Id-1 site-directed mutants were generated using a site-directed mutagenesis kit (Stratagene, La Jolla, CA) with procedures described by the manufacturer. The resulting constructs were confirmed by sequencing and then transfected into cells using FuGENE 6 reagent (Roche Diagnostics). The Si-Con, Si-Id-1, and Si-Cav-1 were synthesized commercially by siGENOME™ (Dharmacon). The targeting sense sequences are as follows: *Si-ID-1*, UAAACGUGCUGCUCUACGA; *Si-CON*, UAAGGCUAUGAAGAGAUAC; *Si-CAV-1* (a mixture of 4): Si-Cav-1-1, CUAAACACCUCAACGAUGA; Si-Cav-1-2, GCAAAUACGUAGACUCGGA; Si-Cav-1-3, GCAGUUGUACCAUGCAUUA; and Si-Cav-1-4, GCAUCAACUUGCAGAAAGA (ON-TARGET plus SMARTpool Human Cav-1). They were transiently transfected into cells with Lipofectamine according to the protocols described before (21).

Western Blotting—Detailed experimental procedures were described previously (21). The primary antibodies used were as follows: Id-1, Cav-1, N-cadherin, β-actin (Santa Cruz Biotechnology), E-cadherin, α-catenin, β-catenin, GSK3β (BD Biosciences), p-Akt, Akt, p-GSK3β (Cell Signaling Technology), α-SMA, vimentin, FLAG, HA (Sigma), and PP2A-C subunit (Upstate Biotechnology, Inc.).

Immunoprecipitation—Cells were lysed in RIPA buffer 48 h after transfection. Immunoprecipitation was performed with the FLAG HA tandem affinity purification kit (Sigma). Briefly, cell lysates were incubated with anti-FLAG M2 affinity resin or anti-HA-agarose affinity resin overnight. The resin was then washed three times with lysis buffer. The complex on the anti-FLAG M2 affinity resin was eluted with 3×FLAG peptide (150 ng/ml), and the complex on anti-HA-agarose affinity resin was eluted with urea (8 M) for 30 min at 4 °C. The eluted complex was loaded onto SDS-PAGE for Western blotting analysis, using the procedures described above.

For endogenous immunoprecipitation, cell lysate was precleared by incubation with protein G-agarose beads and rabbit IgG for 1 h at 4 °C and then incubated with anti-Cav-1 (Santa Cruz Biotechnology) overnight at 4 °C. The protein G-agarose beads were then added into the cell lysate and further incubated for 2 h. The beads were then washed with RIPA buffer and boiled with 2× sample buffer for 10 min at 100 °C. The supernatant was loaded onto as SDS-PAGE for Western blotting analysis.

RT-PCR—Total RNA was isolated from cells using TRIzol reagent according to the manufacturer's protocol (Invitrogen). For RT-PCR, cDNAs were synthesized using the SuperScript™ first strand synthesis system (Invitrogen) and then amplified by PCR with *E-cadherin*-specific primers as described previously (26). The PCR conditions were as follows: an initial denaturation at 95 °C was followed by 28 cycles of PCR (94 °C for 1 min, 56 °C for 1 min, and 72 °C for 1 min) and a final extension at 72 °C for 5 min. *GAPDH* was amplified as an internal loading control. PCR products were electrophoresed on 1.5% agarose gels and analyzed using a gel documentation system (UVP, LLC, Upland, CA).

Luciferase Assay—Cells were plated into a 24-well plate at a density of 5×10^4 cells per well and were co-transfected with pGL2-Basic-Ecad1359 (kindly provided by Dr. Karen M. Habra and Dr. Amy S. Woodard, Departments of Internal Medicine, Human Genetics, and Pathology, University of Michigan Medical School) (27), pRL-CMV-Luc (internal control), WT-Id-1, or truncated Id-1 (FLAG-CT60-Id-1) and Cav-1, respectively. After 48 h, the cells were lysed and assayed for luciferase activity using the dual-luciferase reporter assay system (Promega, WI). Each data point represents the mean of three experiments, and error bars indicate the standard deviation.

3-(4,5-Dimethylthiazol-2-yl)-2,5-diphenyltetrazolium Bromide (MTT) Assay—Cell viability was measured using a MTT proliferation assay kit, and the detailed procedures were described previously (21).

Immunofluorescent Staining—Cells were fixed with 4% paraformaldehyde and washed with 1× phosphate-buffered saline. The cells were incubated with a primary polyclonal antibody against Id-1, a TRITC-labeled secondary antibody against rabbit IgG (DakoCytomation), a primary monoclonal antibody against Cav-1 (BD Biosciences), and a fluorescein isothiocyanate-labeled secondary antibody against mouse IgG (DakoCytomation), respectively, or the cells were incubated with primary antibodies against E-cadherin or β-catenin (BD Biosciences), respectively, and then were incubated with a fluorescein isothiocyanate-labeled secondary antibody against mouse IgG (DakoCytomation). Signals were visualized and captured using a fluorescent microscope under ×400 magnifications.

Wound Closure Assay—Detailed experimental procedures were described previously (26). Cell migration rate was generated as follows. The vertical distance between two borderlines of the wound was measured, and the distance was set up as 1.0 at time 0 h in each cell line. Cell migration rate was calculated by dividing the distance between two borderlines at indicated experimental time points and time 0 h.

Protein Phosphatase 2A Activity Assay—The PP2A activity was measured using a PP2A immunoprecipitation phosphatase assay kit with the procedures described by the manufacturer (Upstate Biotechnology, NY). Briefly, cells were lysed with phosphatase lysis buffer described as before (28) and incubated with a monoclonal antibody against PP2A-C subunit and the protein A-agarose slurry for 1 h. The agarose beads were then washed twice with phosphatase lysis buffer and once with phosphatase assay buffer. PP2A activity was determined using a malachite green phosphatase assay protocol with a phosphopeptide (KRpTIRR) as the substrate, followed by the measurement of absorbance at 650 nm. Results represented the OD ratio between the transfected cells and the untransfected controls. Each data point represented the mean ± S.D.

RESULTS

Identification of an Id-1 Interacting Protein, Caveolin-1—To identify novel Id-1 interacting proteins, we used a full-length Id-1 cDNA as a bait to screen a cDNA library derived from an immortalized human nonmalignant prostatic epithelial cell line, Hpr-1, using the yeast two-hybrid technique. Sixteen positive clones were selected (data not shown). Sequence analysis and data base comparison revealed that one positive clone had 100% identity to the *Homo sapiens* caveolin-1 mRNA coding sequence (GenBank™ accession number NM_001753). It encodes a cell membrane protein, caveolin-1 (Cav-1), a subunit of caveolins that are necessary for caveolae formation, and has been reported to regulate the signaling of membrane proteins such as epidermal growth factor receptor, Src, and H-ras through direct physical interaction (23). Previously, it has been reported that similar to the Id-1 expression patterns in prostate cancer (5, 29, 30), Cav-1 is up-regulated in metastatic prostate cancer specimens, and its expression levels are correlated positively with Gleason Score (31). Therefore, we hypothesized that interaction between Id-1 and Cav-1 may play a role in mediating the oncogenic function of Id-1 in prostate cancer.

To confirm the *in vivo* interaction between Id-1 and Cav-1, expression vectors containing Id-1-FLAG and Cav-1-HA were co-transfected into a prostate cancer cell line, LNCap, and the cells transfected with Cav-1-HA alone were used as a negative control. As shown in Fig. 1*A*, Western blotting analysis on total cell lysates showed that HA was detected in the cells transfected with Cav-1-HA (Fig. 1*A*, *lane 1, upper panel*), whereas both HA and FLAG were detected in the cells transfected with Id-1-FLAG + Cav-1-HA (*lane 2*), indicating successful expression of both proteins. After immunoprecipitation with anti-FLAG M2 affinity resin, Cav-1-HA was detected in the precipitates derived from the cells co-transfected with both Id-1-FLAG and Cav-1-HA (Fig. 1*A*, *lane 4*), indicating co-immunoprecipitation of Cav-1 with Id-1. Reciprocally, after immunoprecipitation with anti-HA-agarose affinity resin (Fig. 1*A*, *lower panel*), Id-1-FLAG was detected in the cells co-transfected with the two proteins (*lane 8*), confirming the interaction between Cav-1 and Id-1. To confirm these results, two prostate cancer cell lines with relatively high levels of Id-1 and Cav-1 were used to repeat the immunoprecipitation experiments (Fig. 1*B*, *left panel*). As shown in Fig. 1*B* (*lanes 3* and *6*), the endogenous Id-1 was detected in the immunoprecipitates by an anti-

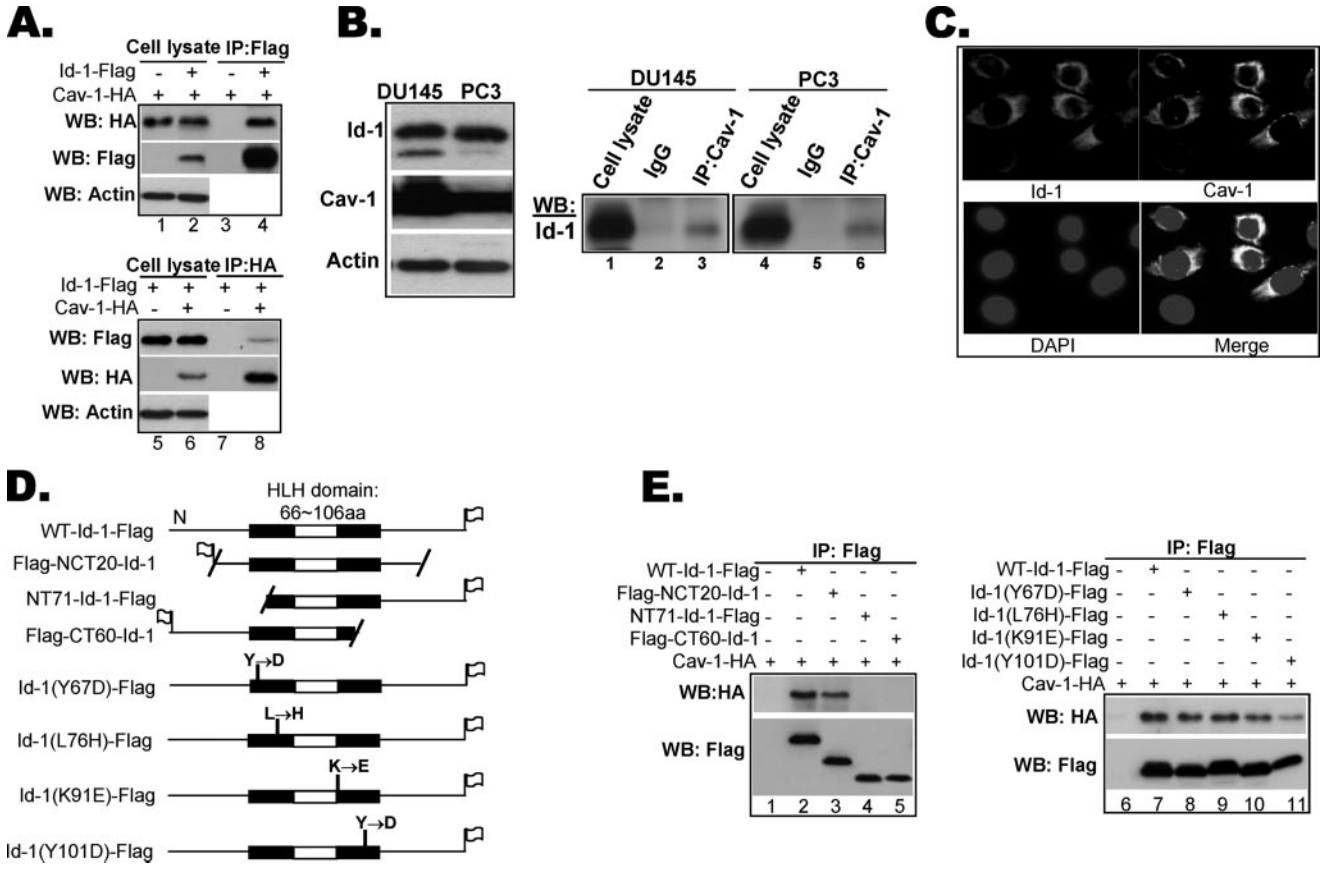

FIGURE 1. **Id-1 interacts with Cav-1.** *A,* co-immunoprecipitation analysis of Id-1 and Cav-1 in LNCap cells. Expression vectors containing ID-1-FLAG and *CAV-1-HA* were co-transfected into LNCap cells, and cells transfected with *CAV-1-HA* or *ID-1-FLAG* alone were used as negative controls, respectively. Cell lysates were immunoprecipitated (*IP*) with anti-FLAG affinity resin and blotted with anti-HA and anti-FLAG (*top panel*) or anti-HA-agarose affinity resin and blotted with anti-FLAG or anti-HA (*bottom panel*), respectively. Note that Cav-1-HA co-immunoprecipitates with Id-1-FLAG (*lane 4, upper panel*), and vice versa (*lane 8, bottom panel*). *B,* immunoprecipitation analysis of endogenous Id-1 and Cav-1 in DU145 and PC3 cells. *Left panel,* Western blotting (*WB*) analysis of Id-1 and Cav-1 expression. *Right panel,* Western blotting analysis of Id-1 expression in cell lysate immunoprecipitated with an anti-Cav-1 antibody. *C,* immunofluorescent staining of Id-1 and Cav-1. Hpr1 cells were fixed and stained with anti-Id-1 rabbit polyclonal antibody and anti-Cav-1 mouse monoclonal antibody and processed for fluorescent microscope imaging. *Top left*, immunofluorescent staining shows cytoplasmic localization of Id-1; *top right*, immunofluorescent staining shows the localization of Cav-1, and the *bottom left* shows cell nuclear staining by 4′,6-diamidino-2-phenylindole (*DAPI*). Merged fluorescent image indicates cytoplasmic co-localization of Id-1 and Cav-1. Photos were taken under ×400 magnifications. *D,* structure of FLAG-tagged truncated and mutated Id-1 constructs. Three truncated Id-1s, FLAG-NCT20-Id-1 (20 amino acids deleted from N- and C-terminals), NT71-Id-1-FLAG (71 amino acids deleted from N terminus), and FLAG-CT60-Id-1 (60 amino acids deleted from C terminus), and four Id-1 mutants, Id-1(Y67D)-FLAG, Id-1(L76H)-FLAG, Id-1(K91E)-FLAG, and Id-1-(Y101D)-FLAG, were generated. *E,* co-immunoprecipitation analysis of Id-1 mutants and Cav-1. Expression vectors containing FLAG-tagged truncated or point-mutated *ID-1* and *CAV-1-HA* were co-transfected into LNCap cells, and cell lysates were immunoprecipitated with anti-FLAG affinity resin and blotted with anti-HA and anti-FLAG, respectively. Note that Cav-1-HA only co-immunoprecipitates with FLAG-NCT20-Id-1 (*lane 3, upper panel*) and FLAG tagged WT-Id-1 (*lane 2 upper panel*), whereas all the FLAG-tagged point-mutated Id-1s co-immunoprecipitate with Cav-1-HA (*lanes 7–11, upper panel*).

Cav-1 antibody in both cell lines, further suggesting an interaction between these two proteins. In addition, fluorescent immunostaining also showed that both Id-1 and Cav-1 were co-localized in the cytoplasm of Hpr-1 cells (Fig. 1*C*). Taken together, these results suggest a physical interaction between Id-1 and Cav-1.

To identify the binding domain of Id-1 to Cav-1, we constructed three vectors expressing truncated forms of Id-1, FLAG-NCT20-Id-1 (20 amino acids deleted from N and C termini, respectively), NT71-Id-1-FLAG (71 amino acids deleted from N terminus), and CT60-Id-1-FLAG (60 amino acids deleted from C terminus) (Fig. 1*D*). These three *ID-1* truncates and the wild type *ID-1* were then co-transfected, respectively, with *CAV-1-HA* into LNCap cells, and the whole cell extracts were immunoprecipitated with anti-FLAG M2 affinity resin. As shown in Fig. 1*E*, all the FLAG-tagged Id-1 proteins were detected in the precipitates (*lanes 2–5, lower panel*), indicating successful immunoprecipitation of the FLAG protein. The Cav-1-HA, however, was only detected in the cells expressing WT-Id-1-FLAG and FLAG-NCT20-Id-1, which contained an intact HLH domain of the Id-1 protein (Fig. 1*E*, *lanes 2* and *3, upper panel*). These results demonstrate that the HLH domain of the Id-1 protein may be essential for the interaction between Id-1 and Cav-1. To further study the importance of the HLH domain in the binding activity, we constructed four Id-1 mutants containing point mutations, in which one of the conserved amino acids in the HLH domain was mutated (Fig. 1*D*). Then these mutants were co-transfected, respectively, with Cav-1-HA into LNCap cells, and immunoprecipitation was performed using anti-FLAG M2 affinity resin. As shown in Fig. 1*E*, Cav-1-HA was detected in all of the precipitates (*lanes 7–11, upper panel*), indicating that one amino acid alteration in the HLH domain is not sufficient to completely destroy the binding activity of Id-1 to Cav-1. However, the binding between

Id-1(Y101D)-FLAG and Cav-1-HA seemed much weaker than the wild type Id-1 and the other mutants, suggesting that the Tyr-101 amino acid may be important for the binding activity of Id-1 to Cav-1. Taken together, these results suggest that the HLH domain of Id-1 is essential for its interaction with Cav-1, and that point mutations in the HLH domain are not sufficient to completely abolish its binding activity to Cav-1.

Interaction between Id-1 and Cav-1 Is Essential for Id-1-induced EMT—It has been reported that both Id-1 and Cav-1 play a positive role in metastatic progression of prostate cancer (30, 32). It is possible that the interaction between these two proteins may play a role in their effect on the invasion ability of prostate cancer cells. Therefore, we next studied the significance of Id-1-Cav-1 interaction in mediating Id-1-induced EMT, a shift in protein expression from epithelial to mesenchymal markers and a key process in promoting invasion and metastasis of cancer cells (33). Two prostate cancer cell lines, LNCap and 22RV1, were used in this study because Id-1 expression could be modified with different culture conditions. Under serum-free culture conditions, these two lines showed low or undetectable Id-1 and Cav-1 expression so that the effect of ectopic expression of both proteins could be studied. As shown in Fig. 2*A*, WT-Id-1 + Cav-1, FLAG-CT60-Id-1 (the no-binding Id-1 mutant) + Cav-1, as well as Id-1 or Cav-1 alone controls were successfully transfected into these two cell lines. Then the expression levels of three epithelial markers, E-cadherin, α-catenin, and β-catenin, and three mesenchymal markers, N-cadherin, α-smooth muscle actin, and vimentin, were examined by Western blotting. As shown in Fig. 2*B*, *WT-ID-1* and *CAV-1* transfection alone were able to modify the expression of both epithelial markers and mesenchymal markers (*lanes 1 versus 2* or *3* for LNCap; *lanes 6 versus 7* or *8* for 22RV1), suggesting that each of them alone is able to promote EMT. However, in the cells transfected with *WT-ID-1 + CAV-1*, the decreased expression of epithelial markers, especially E-cadherin and α-catenin, and increased expression of mesenchymal markers, especially N-cadherin and vimentin, were much more significant (highlighted) compared with either the control (Fig. 2*B*, *lane 1*) or the cells transfected with *ID-1* (*lanes 2* and *7*) or *CAV-1* (*lanes 3* and *8*) alone. In contrast, this effect was partially reversed in the cells transfected with *CT-60-ID-1 + CAV-1* (Fig. 2*B*, *lanes 4 versus 5*

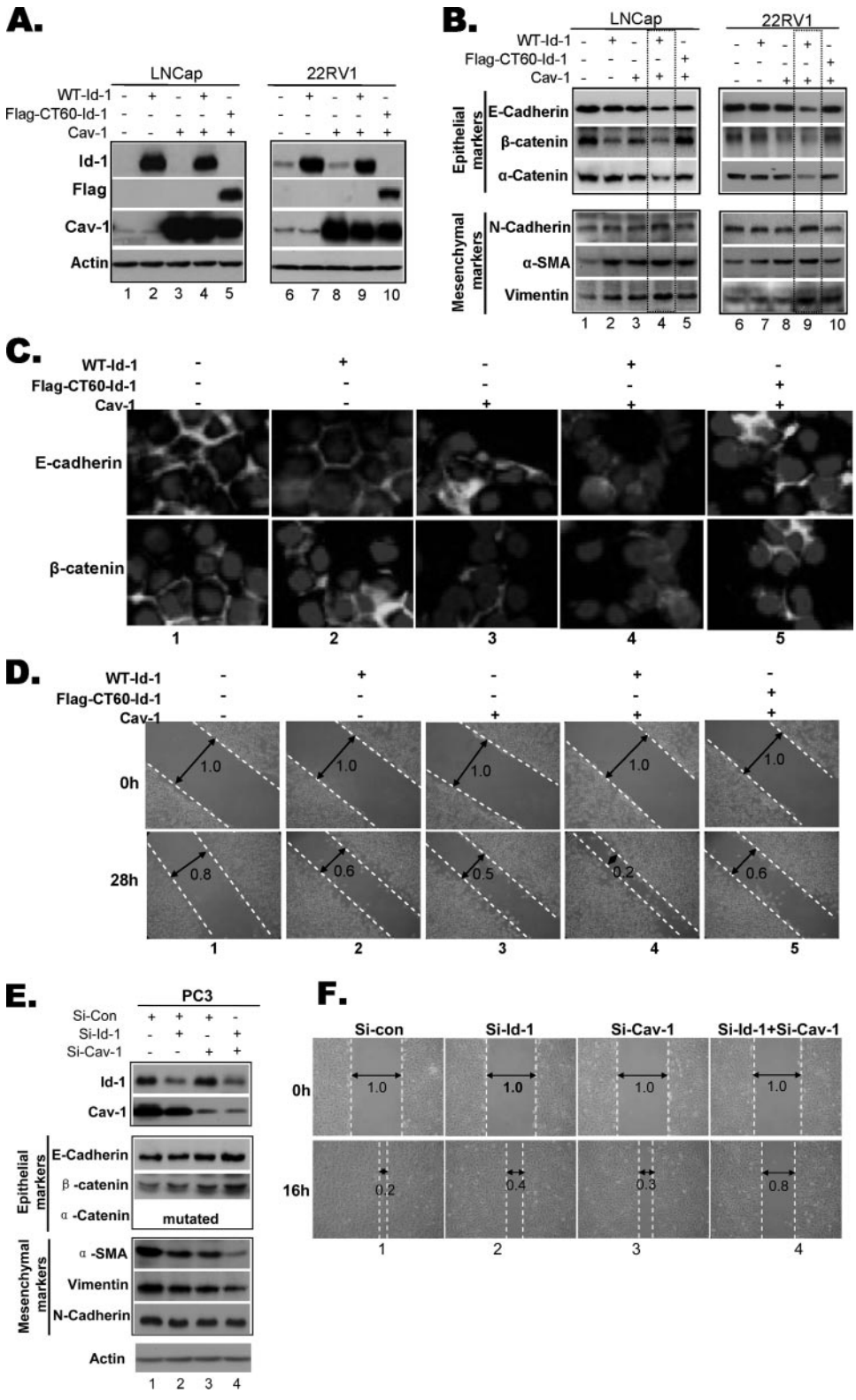

and *9 versus 10*). These results indicate that the interaction between Id-1 and Cav-1 is important for a synergistic effect on promoting EMT.

Because the membrane localization of cell adhesion molecules such as E-cadherin is essential for its biological function (35), next we performed immunofluorescent staining to examine the re-distribution of E-cadherin and its membrane complex β-catenin. As shown in Fig. 2*C*, E-cadherin and β-catenin staining was detected mainly in the cytoplasm of the cells transfected with *WT-ID-1 + CAV-1* (*panel 4*), whereas positive staining was found in the cell membrane region in vector control cells (*panel 1*) and cells transfected with *ID-1* (*panel 2*) or *CAV-1* (*panel 3*) alone. In the FLAG-CT60-Id-1 + Cav-1 transfectants (Fig. 2*C*, *panel 5*), membrane staining was also detected. These results indicate that the interaction between Id-1 and Cav-1 may be able to promote subcellular re-distribution of E-cadherin and β-catenin proteins. To study if the Id-1 + Cav-1-induced EMT played a positive role on cell migration, we performed wound closure assay. As shown in Fig. 2*D*, the WT-Id-1 + Cav-1 transfectants showed the fastest migration rate, evidenced by the lowest distance ratio between wound gap at the 28- and 0-h experimental time point (*panel 4*, distance ratio to 0 h = 0.2) among all the cell lines (*panels 1–3*, distance ratio to time 0 h ≥0.5). However, the migration rate was lower in the cells transfected with FLAG-CT60-Id-1 + Cav-1 (*panel 5*; distance ratio to time 0 h = 0.6). These results suggest that the Id-1-induced cell migration ability is enhanced through its interaction with Cav-1.

To further confirm the effect of Id-1 and Cav-1 on EMT and cell migration, the expression of Id-1 and Cav-1 was down-regulated using small interfering RNA technology, and the effect on EMT and cell migration was studied on the PC3 cell line that showed relatively high levels of both proteins (Fig. 1*B*, *left panel*). After transfecting with *si-ID-1 + si-CAV-1* (Fig. 2*E*, *lane 4*), the expression of epithelial markers was increased compared with the cells transfected with *si-ID-1* (*lane 2*) or *si-CAV-1* (*lane 3*) alone or *si-CON* (*lane 1*), which was correlated with decreased expression of mesenchymal markers especially α-SMA and vimentin, suggesting that down-regulation of Id-1 and Cav-1 is able to reverse their positive effect on EMT. In addition, as shown in Fig. 2*F*, the si-Id-1 + si-Cav-1 transfectants showed the slowest migration rate (*panel 4*, distance ratio to time 0 h = 0.8) compared with the cells transfected with *si-ID-1* (*panel 2*, distance ratio to 0 h = 0.4), *si-CAV-1* alone (*panel 3*, distance ratio to 0 h = 0.3), or *si-CON* (*panel 1*, distance ratio to 0 h = 0.2), suggesting that suppression of both Id-1 and Cav-1 leads to slower cell migration. These results support the evidence generated from overexpression experiments and further suggest that Id-1 and Cav-1 synergistically promote invasion ability of prostate cancer cells.

To study if the Id-1 + Cav-1-induced E-cadherin down-regulation was regulated at the transcriptional level, we performed RT-PCR and luciferase assay. As shown in supplemental Fig. 1, *A* and *B*, both the mRNA level of E-cadherin and its promoter activity were decreased in the WT-Id-1 + Cav-1 transfectants (*lane 4*) compared with FLAG-CT60-Id-1 + Cav-1 (*lane 5*), the vector control (*lane 1*), the cells transfected with *WT-ID-1* (*lane 2*), or *CAV-1* (*lane 3*) alone, suggesting that interaction between Id-1 and Cav-1 may contribute to transcriptional suppression of E-cadherin expression.

The Id-1 + Cav-1-induced EMT and Invasion Are Mediated through Akt Pathway—Previously, it was reported that activation of Akt through phosphorylation was associated with prostate cancer progression and poor clinical outcome (37, 38). Cav-1, on the other hand, was found to promote Akt activation in prostate cancer cells (39). Therefore, we hypothesized that the Akt pathway may play a role in regulating the synergistic effect of Id-1 and Cav-1 in promoting EMT in prostate cancer cells. To test this hypothesis, we examined the expression of p-Akt and its downstream effector p-GSK3β. As shown in Fig. 3*A*, the expression of both p-Akt and p-GSK-3β was increased moderately in the cells transfected with *ID-1* (*lanes 2* and *7*) or *CAV-1* (*lanes 3* and *8*) alone; however, the expression of both p-Akt and p-GSK-3β was increased significantly in the cells transfected with *WT-ID-1 + CAV-1* (*lanes 4* and *9*, highlighted) compared with the vector control (*lanes 1* and *6*) or the cells transfected with *ID-1* (*lanes 2* and *7*) or *CAV-1* (*lanes 3* and *8*) alone. This effect was not detected in the cells transfected with *FLAG-CT60-ID-1 + CAV-1* (Fig. 3*A*, *lanes 5* and *10*). These results suggest that although overexpression of Id-1 and Cav-1 alone is able to increase the phosphorylation of Akt and GSK-3β, the interaction between Id-1 and Cav-1 synergistically promotes Akt pathway activation. To further confirm the significance of Akt phosphorylation in WT-Id-1 + Cav-1-induced EMT and cell migration, we treated the *WT-ID-1 + CAV-1*-transfected cells with two specific PI3K/Akt inhibitors, wortmannin and LY294002, and we studied their effect on the expression of E-cadherin, β-catenin, α-catenin, as well as N-cadherin and α-SMA. As shown in Fig. 3*B*, the expression of p-Akt and p-GSK-3β was decreased after treatment with wortmannin (100 nM) (*lane 3*) and LY294002 (20 μm) (*lane 5*), respectively, compared with the untreated control (*lanes 2* and *4*). This decrease was associated with increased expression of epithelial markers and down-regulation of mesenchymal markers. In addition, fluorescent immunostaining studies also showed that both wortmannin and LY294002 treatment pro-

FIGURE 2. **Effect of Id-1 and Cav-1 interaction on EMT and cell migration in prostate cancer cells.** LNCap and 22RV1 cells were co-transfected with *WT-ID-1 + CAV-1*, *FLAG-CT60-ID-1* (no-binding Id-1 mutant) + *CAV-1*, as well as the *ID-1*, *CAV-1*, or vector alone controls. 24 h after transfection, medium was changed to serum-free medium for another 24 h. *A,* Western blotting analysis of WT-Id-1, FLAG-CT60-Id-1, and Cav-1 expression in the transfectants. *B,* effect of Id-1 and Cav-1 on the expression of EMT markers by Western blotting. *C,* immunofluorescent staining of E-cadherin and β-catenin in LNCap cells. Photos were taken under ×400 magnifications. *D,* cell migration rate examined by wound closure assay. A scraped wound was introduced on monolayer LNCap cells, and the speed of wound closure was monitored at 28 h. The vertical distance between two borderlines of the wound was measured, and the distance was set up as 1.0 at time 0 h in each cell line. Cell migration rate was calculated by dividing the distance between two borderlines at 28 h time point and time 0 h. Note that transfection of WT-Id-1 + Cav-1 promotes EMT and migration ability of LNCap cells. *E* and *F,* effect of Id-1 and Cav-1 down-regulation on the expression of EMT markers and cell migration rate in PC3 cells. Cells were transiently transfected with *Si-ID-1*, *Si-CAV-1*, *Si-ID-1 + Si-CAV-1*, and *Si-CON*, respectively, for 24 h. Western blotting was performed on cell lysate (*E*). Wound closure assay was performed on the transfectants (*F*). Cell migration rate was calculated as described in *D*.

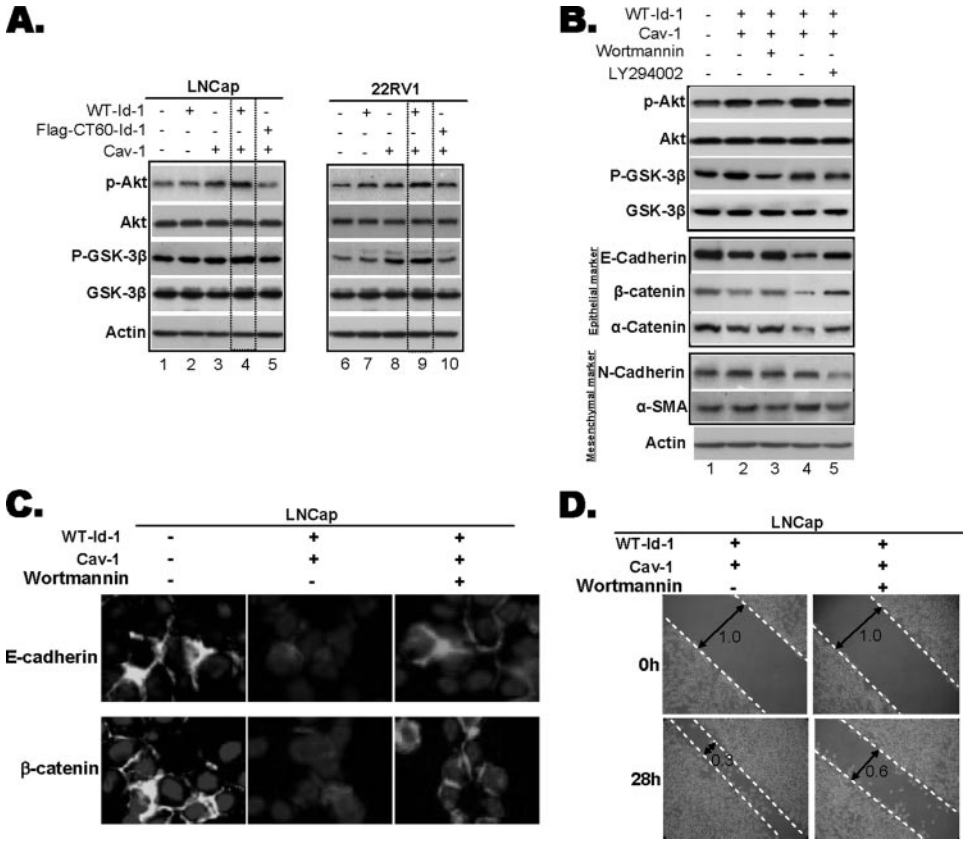

FIGURE 3. **Role of Akt pathway in WT-Id-1 + Cav-1-induced EMT and cell migration in prostate cancer cells.** LNCap cells were transfected with *WT-ID-1 + CAV-1*, *FLAG-CT60-ID-1*, *CAV-1*, and empty vector, and 24 h after transfection, the medium was changed to serum-free medium for 24 h. *A*, Western blotting analysis of the expression of p-Akt and p-GSK3β. *B*, Western blotting analysis of Akt and GSK expression and EMT markers in the cells treated with PI3K/Akt-specific inhibitors LY294002 (20 μM) or wortmannin (100 nM). *C*, immunofluorescent staining of E-cadherin and β-catenin before and after exposure to wortmannin (100 nM) in LNCap cells. Photos were taken as described in Fig. 2*C*. *D*, effect of PI3K/Akt-specific inhibitor wortmannin (100 nM) on cell migration. Note that Akt pathway activation is associated with EMT and increased cell migration, which can be suppressed by PI3K/Akt-specific inhibitors.

moted re-distribution of E-cadherin and β-catenin to cell membrane (representative results on wortmannin-treated cells are shown in Fig. 3*C*). Furthermore, the speed of cell migration was also reduced in the wortmannin-treated cells (Fig. 3*D*). These results suggest that Akt activation plays a key role in the Id-1 + Cav-1-induced EMT and cell migration.

Significance of Interaction between Id-1 and Cav-1 in Protection against Taxol-induced Apoptosis—Previously, Id-1 has been suggested as an anti-apoptotic factor against a variety of anticancer drugs (40). To study if the interaction between Id-1 and Cav-1 played a role in the anti-apoptotic function of Id-1, first, we treated the LNCap and 22RV1 transfectants with taxol and examined cell viability by MTT assay. As shown in Fig. 4*A*, after being exposed to three doses of taxol, different cell viability was observed in the cells transfected with *WT-ID-1 + CAV-1* (*black columns*) compared with the vector control (*open columns*) and the cells transfected with *ID-1* (*columns* with *horizontal lines*) or *CAV-1* (*columns* with *vertical lines*) alone. The percentage of viable cells was the highest in the WT-Id-1 + Cav-1 transfectants (Fig. 4*A*, *black columns*), and the difference reached statistical significance in the cells treated with two high doses of taxol compared with the other cell lines (*, $p < 0.05$). In contrast, the FLAG-CT60-Id-1 + Cav-1 transfectants (Fig. 4*A*, *columns* with *diagonal lines*) showed a lower cell viability compared with the cells transfected with *WT-ID-1 + CAV-1* (*black columns*, *, $p < 0.05$), but no significant difference was found when compared with the cells transfected with *ID-1* or *CAV-1* alone ($p > 0.05$). These results indicate that the interaction between Id-1 and Cav-1 seems to provide a survival benefit in response to taxol in prostate cancer cells.

Activation of the Akt pathway is reported to promote cell survival through protection against chemotherapeutic drug-induced apoptosis (41). Next, we studied if the WT-Id-1 + Cav-1-induced Akt activation played a role in protection against taxol-induced apoptosis in both cell lines. As shown in Fig. 4*B*, after taxol treatment, the cells transfected with *WT-ID-1 + CAV-1* (*lanes 4* and *9*, *highlighted*) showed higher levels of p-Akt compared with the vector control (*lanes 1* and *6*) and the cells transfected with *ID-1* (*lanes 2* and *7*) or *CAV-1* (*lanes 3* and *8*) alone, which was correlated with higher expression of Bcl-2 and decreased expression of cleaved-caspase 3 and PARP. However, this effect was partially reversed in the cells transfected with FLAG-CT60-*ID-1 + CAV-1* (Fig. 4*B*, *lanes 5* and *10*). These results suggest that activation of Akt is associated with resistance to taxol-induced apoptosis in the WT-Id-1 + Cav-1 transfectants. To further confirm the importance of the Akt pathway, we treated the WT-Id-1 + Cav-1 cells with two PI3K/Akt inhibitors, LY294002 and wortmannin, and we studied whether inhibition of PI3K/Akt pathway could promote taxol-induced apoptosis. As shown in Fig. 4*C*, suppression of Akt phosphorylation (*lanes 4* and *8*) resulted in promotion of caspase 3 and PARP cleavage and suppression of Bcl-2 expression (*lanes 4 versus 3* and *lanes 8 versus 7*), and decreased cell viability in the *WT-ID-1 + CAV-1*-transfected cells (Fig. 4*D*, *, $p < 0.05$). These results demonstrate that Akt pathway activation plays a key role in the WT-Id-1 + Cav-1-induced protection against taxol-induced apoptosis.

Id-1 Inhibits PP2A Activity through Interaction with Cav-1—Previously, it has been reported that Cav-1 promotes Akt activation through suppression of the activity of two serine/threonine protein phosphatases, PP1 and PP2A, by forming direct physical interaction (39). Next, we investigated if the WT-Id-1 + Cav-1-induced Akt activation was mediated through modification of PP2A activity. As shown in Fig. 5*A*, the PP2A activity was lower in the Cav-1-transfected cells compared with the control (*columns 3*

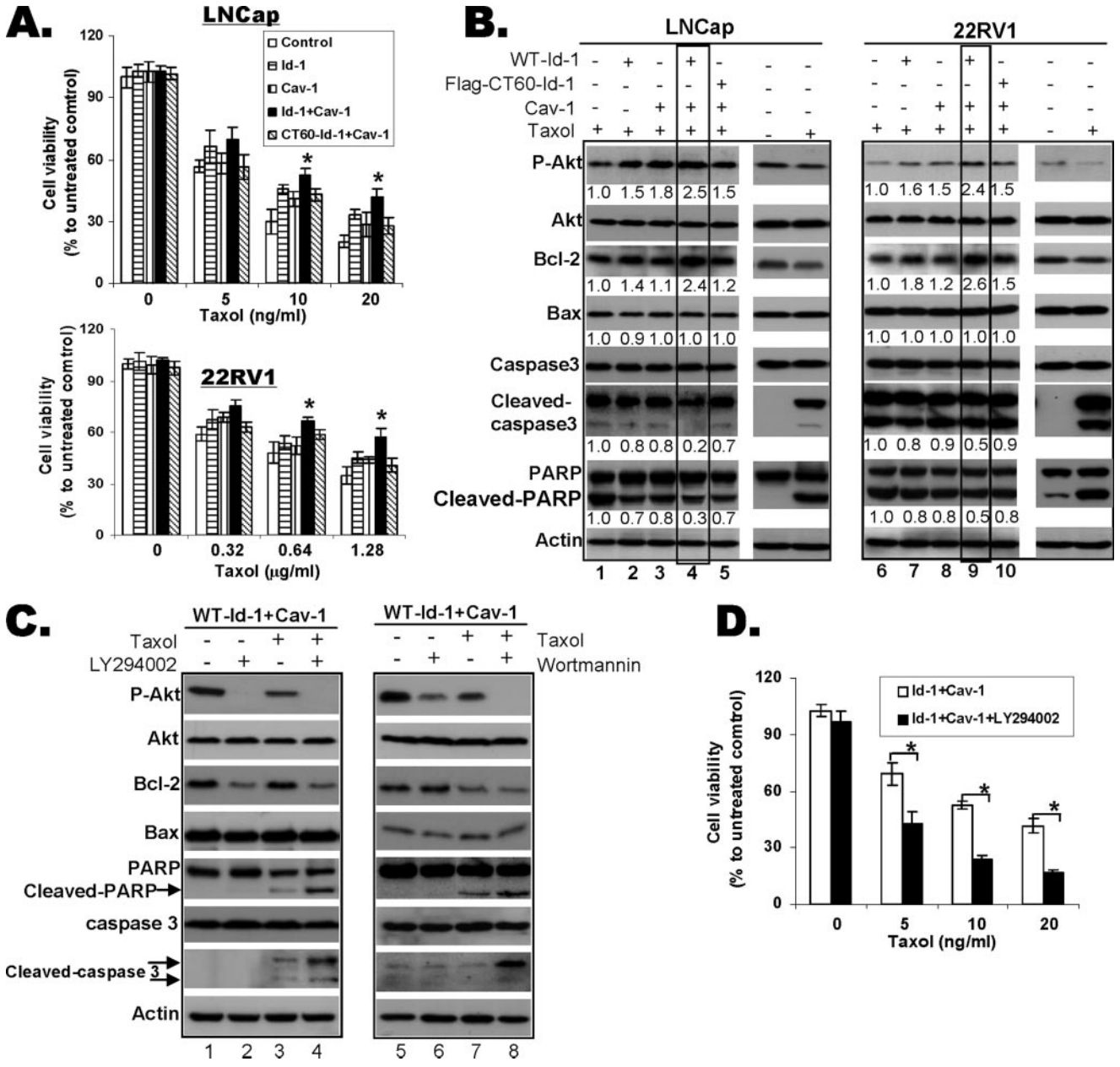

FIGURE 4. **Effect of Id-1 and Cav-1 on taxol-induced apoptosis in prostate cancer cells.** Cells were co-transfected with *WT-ID-1 + CAV-1*, *CT60-ID-1 + CAV-1*, as well as *ID-1* or *CAV-1*, vector alone controls for 24 h. *A*, cell viability of LNCap and 22RV1 after exposure to taxol examined by MTT assay. 24 h after transfection, cells were seeded in 96-well plates and cultured for 24 h and then treated with three doses of taxol in serum-free medium, respectively, for 24 h. Note that cell viability is higher in the WT-Id-1 + Cav-1 transfectants (*, $p < 0.05$). *B*, Western blotting analysis of Akt and apoptosis-related proteins after exposed to taxol (10 ng/ml for LNCap and 50 ng/ml for 22RV1). After transfection for 24 h, the cells were treated with taxol in serum-free medium for another 24 h. Note that the expression of Bcl-2 is much higher in the cells transfected with *WT-ID-1 + CAV-1*, which is associated with decreased expression of cleaved caspase 3 and PARP, compared with the cells transfected with *ID-1* or *CAV-1* alone and the vector control. The relative intensity of each band was quantified using the taxol-treated untransfected cells as a control, which was set up as 1.0. The results are shown as the ratios between the transfected and the untransfected cells indicated at the *bottom* of each gel. *C*, Western blotting analysis of the expression of apoptosis-related proteins after exposure to PI3K/Akt-specific inhibitors LY294002 (*left panel*) or wortmannin (*right panel*) in the WT-Id-1 + Cav-1 transfectants. Note that the expression of p-Akt is decreased after treatment with wortmannin (100 nM) and LY294002 (20 μM) compared with the untreated control, which is associated with the increased expression of cleaved caspase 3 and PARP. *D*, cell viability of LNCap cells transfected with WT-Id-1 + Cav-1 after exposure to taxol and LY294002 (20 μM) examined by MTT assay. Note that cell viability is lower in the cells treated with both LY294002 and taxol compared with the cells treated with taxol alone (*, $p < 0.05$).

versus 1), suggesting that Cav-1 is able to inhibit PP2A activity in prostate cancer cells as reported previously (39). In addition, in WT-Id-1 + Cav-1 transfectants (Fig. 5*A*, *columns 4* and *8*), the PP2A activity was decreased further compared with the vector control (*columns 1* and *5*) and the cells transfected with *ID-1* (*columns 2* and *6*) or *CAV-1* (*columns 3* and *7*) alone (*, $p < 0.05$), suggesting that Id-1 promotes the inhibitory effect of Cav-1 on PP2A. However, decreased PP2A activity was not the result of alteration at PP2A protein expression levels (Fig. 5*A*, *inserted blots*). To study whether the decreased PP2A activity in the WT-Id-1 + Cav-1 transfectants was mediated through a physical interaction between PP2A and the Id-1-Cav-1 complex, we performed immunoprecipitation. As shown in Fig. 5*B*, PP2A was not precipitated with Id-1 when the cells were transfected with Id-1-FLAG

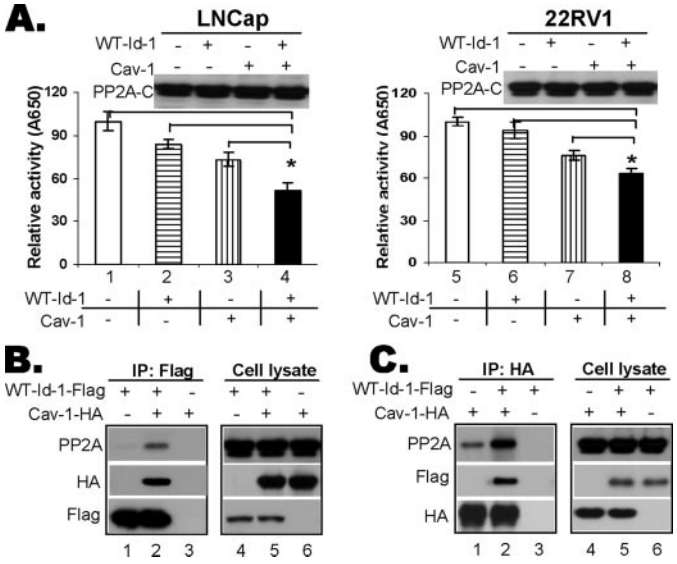

FIGURE 5. **Effect of Id-1 on PP2A activity and its interaction with Cav-1.** *A,* PP2A activity assay. Note that the activity of PP2A is significantly decreased in the cells transfected with *WT-ID-1 + CAV-1* compared with the cells transfected with Id-1 or Cav-1 alone and the vector control (*, $p < 0.05$). *B,* immunoprecipitation analysis of interaction between Id-1 and PP2A. Cell lysates were immunoprecipitated with anti-FLAG and blotted with anti-PP2A, anti-HA, and anti-FLAG, respectively. *C,* immunoprecipitation analysis of interaction between Cav-1, Id-1, and PP2A in LNCap cells. Cell lysates were immunoprecipitated (*IP*) with anti-HA and blotted with anti-PP2A, anti-HA, and anti-FLAG, respectively.

alone (*lane 1*), suggesting that there is no interaction between Id-1 and PP2A in the absence of Cav-1. However, PP2A was detected in the immunoprecipitates when the cells were transfected with *WT-ID-1-FLAG + CAV-1-HA* (Fig. 5*B*, *lane 2*), suggesting interaction between Id-1 and PP2A is mediated through its binding to Cav-1. When we performed immunoprecipitation with anti-HA (Fig. 5*C*), both PP2A and Id-1-FLAG proteins were detected in the cells transfected with *WT-ID-1-FLAG + CAV-1-HA* (*lane 2*), suggesting again a physical interaction between PP2A and Id-1-Cav-1 complex. Most importantly, the PP2A level was much higher in the WT-Id-1 + Cav-1 transfectants (Fig. 5*C*, *lane 2*) compared with the cells transfected with Cav-1-HA alone (Fig. 5*C*, *lane 1*). These results suggest that Id-1 promotes the binding activity between Cav-1 and PP2A, which may lead to suppression of PP2A activity.

DISCUSSION

In this study, we identified a novel Id-1 interacting protein, Cav-1, and found that the HLH domain of Id-1 was essential for its binding to Cav-1. In addition, we demonstrated that interaction between Id-1 and Cav-1 was crucial in promoting Id-1-induced EMT and protection against apoptosis in prostate cancer cells. Furthermore, our results suggest that activation of the Akt pathway through the Id-1-enhanced binding activity between Cav-1 and PP2A may be responsible for the synergistic effect of these two proteins. Our results demonstrate Cav-1 as a direct mediator of Id-1 signaling and provide a novel mechanism responsible for the role of Id-1 in promoting cancer cell invasion and survival.

In addition to its well established function as a dominant negative regulator of binding between bHLH proteins and their targets in muscle cell differentiation (42), recent studies have demonstrated that Id-1 can also bind to and alter the activities of several regulatory proteins. For example, it is reported that Id-1 binds to Ets2, a downstream effector of the MAPK pathway, and inhibits its transcription activity on $p16^{INK4a}$, leading to inhibition of replicative senescence in young human diploid fibroblasts (9). In addition, Id-1 is found to physically interact with several members of the Pax transcription factor family, leading to a loss of DNA binding by Pax proteins and hence down-regulation of the activity of their target promoters (43). In this study, we identified a novel Id-1-interacting non-HLH protein, Cav-1, a primary cell membrane protein and a subunit of caveolae that functions both in protein trafficking and signal transduction, as well as in cholesterol homeostasis (23). The association between caveolins and cancer dates back to the discovery of caveolin-1 as a predominant phosphoprotein in v-*src*-transformed embryonic chicken fibroblasts (44). Since then, a number of reports have demonstrated that *CAV-1* is not only a target of many oncogenes such as c-*MYC*, H-*RAS*, v-*ABL* but is also a regulator of multiple signaling pathways through physical interaction with epidermal growth factor receptor, MEK/ERK, and Ras-p42/44 MAPKs (23). Although it has been suggested as a tumor suppressor in several tumor types (45–47), in prostate cancer *CAV-1* is indicated to be an oncogene (31). Interestingly, similar expression patterns were also observed in Id-1 protein in prostate cancer (5, 29, 30). In this study, our evidence that interaction between Id-1 and Cav-1 was essential to promote Id-1-induced EMT and resistance to apoptosis in prostate cancer cells suggests that Cav-1 may be a mediator of Id-1 signaling in promoting tumorigenesis. In agreement with a previous study (43), we also found that the HLH domain of Id-1 was essential for the physical interaction between Id-1 and Cav-1 (Fig. 1*E*, *left panel*); however, single point mutations of the HLH domain were not sufficient to abolish the binding activity between these two proteins (Fig. 1*E*, *right panel*), suggesting the integrity of the HLH domain is important for the physical interaction between Id-1 and Cav-1. However, unlike the previously reported dominant negative effect of Id-1 on the transcription activity of its binding partners (42), the interaction between Id-1 and Cav-1 led to activation of the Akt pathway and promotion of EMT in prostate cancer cells (Figs. 2 and 4).

Activation of Akt pathway is one of the most frequently reported phenotypes in advanced cancers (41). In this study, our results that the Id-1-induced EMT and protection against apoptosis was mediated through activation of the Akt pathway (Figs. 2–4) suggest a novel molecular pathway that regulates the oncogenic effect of Id-1. As discussed previously, activation of Akt pathway is reported to play a positive role in the progression of prostate cancer (37, 38). It is possible that high levels of Id-1 in the advanced prostate cancer cells may lead to promotion of Akt activation, which provides a survival advantage for cancer progression. In addition, in this study, we also found that interaction between Id-1 and Cav-1 was essential for the Id-1-induced Akt activation (Fig. 3*A*). Because Cav-1 expression is also reported to be associated with progression of prostate cancer (31), it is tempting to speculate that the presence of high levels of Id-1 and Cav-1 in prostate cancer cells may be able to form a complex that may facilitate activation of the Akt pathway. This hypothesis is supported by our evidence that the WT-

Id-1 + Cav-1-induced Akt pathway activation is the result of the Id-1 enhanced binding activity between Cav-1 and PP2A (Fig. 5). Previously, it has been reported that Cav-1 activates Akt through inhibition of PP2A activity through physical interaction, which leads to dephosphorylation of p-Akt (39). In this study, we found that Id-1 was able to promote the binding activity between Cav-1 and PP2A leading to synergistic suppression of the phosphatase activity of PP2A (Fig. 5, *B* and *C*), which may in turn result in increased Akt phosphorylation. Because the two prostate cancer cell lines used in this study contained different PTEN status (PTEN is mutated in LNCap cells (48) and 22RV1 contains a wild type PTEN (49)), the WT-Id-1 + Cav-1-induced Akt activation may not be mediated through PTEN-dependent pathways.

Recently, it has been reported that GSK, a tumor suppressor, can be inactivated through phosphorylation by several oncogenic signals, such as PI3K/Akt, MAPK, and Wnt, which leads to EMT and promotion of cell invasion (50). In this study, we also observed an increased expression of p-GSK3β, an indicator of GSK3β inactivation, in the cells transfected with WT-Id-1 + Cav-1 (Fig. 3*A*), and it is possible that the Cav-1-mediated Akt activation in the Id-1-overexpressing cells may also lead to inactivation of GSK3β. Previously, it is suggested that GSK3β inactivation leads to nuclear expression of the E-cadherin suppressor Snail (51). In this study, we found a decreased E-cadherin transcription in the WT-Id-1 + Cav-1 transfectants (supplemental Fig. 1, *A* and *B*), and it is speculated that down-regulation of E-cadherin expression may be the result of Snail activation induced by the decreased GSK3β activity, which in turn may also contribute to Id-1-induced EMT in prostate cancer cells.

In summary, our study demonstrates an Id-1 binding partner, Cav-1, and suggests a novel molecular mechanism that mediates the function of Id-1 in promoting prostate cancer progression through activation of the Akt pathway leading to prostate cancer cell invasion on one hand and resistance to anticancer drug-induced apoptosis on the other hand.

REFERENCES

1. Perk, J., Iavarone, A., and Benezra, R. (2005) *Nat. Rev. Cancer* **5,** 603–614
2. Lin, C. Q., Singh, J., Murata, K., Itahana, Y., Parrinello, S., Liang, S. H., Gillett, C. E., Campisi, J., and Desprez, P. Y. (2000) *Cancer Res.* **60,** 1332–1340
3. Maruyama, H., Kleeff, J., Wildi, S., Friess, H., Buchler, M. W., Israel, M. A., and Korc, M. (1999) *Am. J. Pathol.* **155,** 815–822
4. Schindl, M., Oberhuber, G., Obermair, A., Schoppmann, S. F., Karner, B., and Birner, P. (2001) *Cancer Res.* **61,** 5703–5706
5. Ouyang, X. S., Wang, X., Lee, D. T., Tsao, S. W., and Wong, Y. C. (2002) *J. Urol.* **167,** 2598–2602
6. Schindl, M., Schoppmann, S. F., Strobel, T., Heinzl, H., Leisser, C., Horvat, R., and Birner, P. (2003) *Clin. Cancer Res.* **9,** 779–785
7. Schoppmann, S. F., Schindl, M., Bayer, G., Aumayr, K., Dienes, J., Horvat, R., Rudas, M., Gnant, M., Jakesz, R., and Birner, P. (2003) *Int. J. Cancer* **104,** 677–682
8. Alani, R. M., Young, A. Z., and Shifflett, C. B. (2001) *Proc. Natl. Acad. Sci. U. S. A.* **98,** 7812–7816
9. Ohtani, N., Zebedee, Z., Huot, T. J., Stinson, J. A., Sugimoto, M., Ohashi, Y., Sharrocks, A. D., Peters, G., and Hara, E. (2001) *Nature* **409,** 1067–1070
10. Nieborowska-Skorska, M., Hoser, G., Rink, L., Malecki, M., Kossev, P., Wasik, M. A., and Skorski, T. (2006) *Cancer Res.* **66,** 4108–4116
11. Kondo, M., Cubillo, E., Tobiume, K., Shirakihara, T., Fukuda, N., Suzuki, H., Shimizu, K., Takehara, K., Cano, A., Saitoh, M., and Miyazono, K. (2004) *Cell Death Differ.* **11,** 1092–1101
12. Singh, J., Murata, K., Itahana, Y., and Desprez, P. Y. (2002) *Oncogene* **21,** 1812–1822
13. Ling, M. T., Lau, T. C., Zhou, C., Chua, C. W., Kwok, W. K., Wang, Q., Wang, X., and Wong, Y. C. (2005) *Carcinogenesis* **26,** 1668–1676
14. Wong, Y. C., Wang, X., and Ling, M. T. (2004) *Apoptosis* **9,** 279–289
15. Tsuchiya, T., Okaji, Y., Tsuno, N. H., Sakurai, D., Tsuchiya, N., Kawai, K., Yazawa, K., Asakage, M., Yamada, J., Yoneyama, S., Kitayama, J., Osada, T., Watanabe, T., Tokunaga, K., Takahashi, K., and Nagawa, H. (2005) *Cancer Sci.* **96,** 784–790
16. Fong, S., Itahana, Y., Sumida, T., Singh, J., Coppe, J. P., Liu, Y., Richards, P. C., Bennington, J. L., Lee, N. M., Debs, R. J., and Desprez, P. Y. (2003) *Proc. Natl. Acad. Sci. U. S. A.* **100,** 13543–13548
17. Desprez, P. Y., Lin, C. Q., Thomasset, N., Sympson, C. J., Bissell, M. J., and Campisi, J. (1998) *Mol. Cell. Biol.* **18,** 4577–4588
18. Wiercinska, E., Wickert, L., Denecke, B., Said, H. M., Hamzavi, J., Gressner, A. M., Thorikay, M., ten Dijke, P., Mertens, P. R., Breitkopf, K., and Dooley, S. (2006) *Hepatology* **43,** 1032–1041
19. Cheung, H. W., Ling, M. T., Tsao, S. W., Wong, Y. C., and Wang, X. (2004) *Carcinogenesis* **25,** 881–887
20. Lin, J. C., Chang, S. Y., Hsieh, D. S., Lee, C. F., and Yu, D. S. (2005) *J. Urol.* **174,** 2022–2026
21. Zhang, X., Ling, M. T., Wang, X., and Wong, Y. C. (2006) *Int. J. Cancer* **118,** 2072–2081
22. Ling, M. T., Wang, X., Ouyang, X. S., Xu, K., Tsao, S. W., and Wong, Y. C. (2003) *Oncogene* **22,** 4498–4508
23. Williams, T. M., and Lisanti, M. P. (2005) *Am. J. Physiol.* **288,** C494–C506
24. Choo, C. K., Ling, M. T., Chan, K. W., Tsao, S. W., Zheng, Z., Zhang, D., Chan, L. C., and Wong, Y. C. (1999) *Prostate* **40,** 150–158
25. Ling, M. T., Kwok, W. K., Fung, M. K., Xianghong, W., and Wong, Y. C. (2006) *Carcinogenesis* **27,** 205–215
26. Chu, Q., Ling, M. T., Feng, H., Cheung, H. W., Tsao, S. W., Wang, X., and Wong, Y. C. (2006) *Carcinogenesis* **27,** 2180–2189
27. Hajra, K. M., Ji, X., and Fearon, E. R. (1999) *Oncogene* **18,** 7274–7279
28. Ivaska, J., Nissinen, L., Immonen, N., Eriksson, J. E., Kahari, V. M., and Heino, J. (2002) *Mol. Cell. Biol.* **22,** 1352–1359
29. Yuen, H. F., Chua, C. W., Chan, Y. P., Wong, Y. C., Wang, X., and Chan, K. W. (2006) *Mod. Pathol.* **19,** 931–941
30. Coppe, J. P., Itahana, Y., Moore, D. H., Bennington, J. L., and Desprez, P. Y. (2004) *Clin. Cancer Res.* **10,** 2044–2051
31. Yang, G., Truong, L. D., Wheeler, T. M., and Thompson, T. C. (1999) *Cancer Res.* **59,** 5719–5723
32. Thompson, T. C., Timme, T. L., Li, L., and Goltsov, A. (1999) *Apoptosis* **4,** 233–237
33. Thiery, J. P. (2002) *Nat. Rev. Cancer.* **2,** 442–454
34. Deleted in proof
35. Hazan, R. B., Qiao, R., Keren, R., Badano, I., and Suyama, K. (2004) *Ann. N. Y. Acad. Sci.* **1014,** 155–163
36. Deleted in proof
37. Kreisberg, J. I., Malik, S. N., Prihoda, T. J., Bedolla, R. G., Troyer, D. A., Kreisberg, S., and Ghosh, P. M. (2004) *Cancer Res.* **64,** 5232–5236
38. Malik, S. N., Brattain, M., Ghosh, P. M., Troyer, D. A., Prihoda, T., Bedolla, R., and Kreisberg, J. I. (2002) *Clin. Cancer Res.* **8,** 1168–1171
39. Li, L., Ren, C. H., Tahir, S. A., Ren, C., and Thompson, T. C. (2003) *Mol. Cell. Biol.* **23,** 9389–9404
40. Zhang, X., Ling, M. T., Wong, Y. C., and Wang, X. (2007) *Cancer Sci.* **98,** 308–314
41. Cheng, J. Q., Lindsley, C. W., Cheng, G. Z., Yang, H., and Nicosia, S. V. (2005) *Oncogene* **24,** 7482–7492
42. Norton, J. D. (2000) *J. Cell Sci.* **113,** 3897–3905
43. Roberts, E. C., Deed, R. W., Inoue, T., Norton, J. D., and Sharrocks, A. D. (2001) *Mol. Cell. Biol.* **21,** 524–533
44. Glenney, J. R., Jr., and Zokas, L. (1989) *J. Cell Biol.* **108,** 2401–2408
45. Bagnoli, M., Tomassetti, A., Figini, M., Flati, S., Dolo, V., Canevari, S., and Miotti, S. (2000) *Oncogene* **19,** 4754–4763
46. Aldred, M. A., Ginn-Pease, M. E., Morrison, C. D., Popkie, A. P., Gimm,

O., Hoang-Vu, C., Krause, U., Dralle, H., Jhiang, S. M., Plass, C., and Eng, C. (2003) *Cancer Res.* **63,** 2864–2871
47. Bender, F. C., Reymond, M. A., Bron, C., and Quest, A. F. (2000) *Cancer Res.* **60,** 5870–5878
48. Li, J., Yen, C., Liaw, D., Podsypanina, K., Bose, S., Wang, S. I., Puc, J., Miliaresis, C., Rodgers, L., McCombie, R., Bigner, S. H., Giovanella, B. C., Ittmann, M., Tycko, B., Hibshoosh, H., Wigler, M. H., and Parsons, R. (1997) *Science* **275,** 1943–1947
49. Skjoth, I. H., and Issinger, O. G. (2006) *Int. J. Oncol.* **28,** 217–229
50. Doble, B. W., and Woodgett, J. R. (2003) *J. Cell Sci.* **116,** 1175–1186
51. Zhou, B. P., Deng, J., Xia, W., Xu, J., Li, Y. M., Gunduz, M., and Hung, M. C. (2004) *Nat. Cell Biol.* **6,** 931–940

Identification of a Novel Inhibitor of Differentiation-1 (ID-1) Binding Partner, Caveolin-1, and Its Role in Epithelial-Mesenchymal Transition and Resistance to Apoptosis in Prostate Cancer Cells

Xiaomeng Zhang, Ming-Tat Ling, Qi Wang, Chi-Keung Lau, Steve C. L. Leung, Terence K. Lee, Annie L. M. Cheung, Yong-Chuan Wong and Xianghong Wang

J. Biol. Chem. 2007, 282:33284-33294.
doi: 10.1074/jbc.M705089200 originally published online September 12, 2007
